J Solid State Electrochem (2010) 14:787–795
DOI 10.1007/s10008-009-0846-x

ORIGINAL PAPER

Electrocatalytic oxidation of the antiviral drug acyclovir on a copper nanoparticles-modified carbon paste electrode

H. Heli · M. Zarghan · A. Jabbari · A. Parsaei · A. A. Moosavi-Movahedi

Received: 2 March 2009 / Revised: 28 March 2009 / Accepted: 6 April 2009 / Published online: 7 May 2009

Abstract The electrocatalytic oxidation of acyclovir (Zovirax) on two different copper-based electrodes: copper microparticles- and copper nanoparticles-modified carbon paste electrodes (denoted as micro-CPE and nano-CPE, respectively) was voltammetrically investigated. In the voltammogram recorded using micro-CPE, a single anodic oxidation peak appeared, while nano-CPE resulted in two overlapped anodic peaks. The anodic currents were related to the electrocatalytic oxidation of acyclovir via the electrogenerated active species of Cu(III) with an EC' mechanism. Acyclovir was oxidized with higher rates at low potentials on nano-CPE compared to micro-CPE. This was related to the nanosize effect of copper nanoparticles. The constants of the electrocatalytic oxidation process and the diffusion coefficient of acyclovir were reported. A sensitive and time-saving determination procedure was developed for the analysis of acyclovir and the corresponding analytical parameters were reported. The proposed amperometric method was applied to the analysis of commercial pharmaceutical products (tablets and topical cream) and the results were in good agreement with the declared values.

Keywords Acyclovir · Zovirax · Copper · Nanoparticle · Electrocatalysis · Modified electrode

H. Heli (✉) · A. A. Moosavi-Movahedi
Institute of Biochemistry and Biophysics,
University of Tehran,
P. O. Box: 13145-1384, Tehran, Iran
e-mail: hheli7@yahoo.com

H. Heli
Department of Chemistry, Razi University,
Kermanshah, Iran

M. Zarghan · A. Jabbari
Department of Chemistry, K. N. Toosi University of Technology,
Tehran, Iran

A. Parsaei
Sobhan Chemotherapeutics Co.,
Tehran, Iran

A. A. Moosavi-Movahedi
Institute of Biochemistry and Biophysics, University of Tehran,
Tehran, Iran

Introduction

Cytomegalovirus is the most important pathogen affecting transplant recipients [1]. It is known to cause both direct and indirect effects, including acute and chronic allograft rejection [2]. To prevent the burden of this infection in solid organ transplant patients, antiviral drugs, namely nucleoside analogs, are commonly used for both cytomegalovirus prophylaxis and treatment.

Nucleoside analogs are widely used as inhibitors of human herpes virus (HSV) replication. The antiviral activity of these substances depends on metabolic activation by phosphorylation to their respective mono-, di-, and triphosphates. The preferential initial phosphorylation to the nucleoside monophosphate by viral enzymes is one mechanism of selective antiviral activity.

Acyclovir (acycloguanosine, 9-carboxymethoxymethylguanine; Scheme 1) is the most commonly used guanine analog antiviral drug. It is primarily used for the treatment of herpes simplex as well as herpes zoster (shingles) infections. Other main indications for its use are primary genital herpes, herpetic encephalitis, and varicella zoster virus (VZV) infections in immunosuppressed patients. It can be used topically, intravenously, or preorally, although its oral absorption is only 20%. It offers limited benefit in the topical treatment of recurrent herpes labialis. It is also efficacious in preventing recurrent genital herpes, as well as in preventing HSV infections in renal allograft recipients.

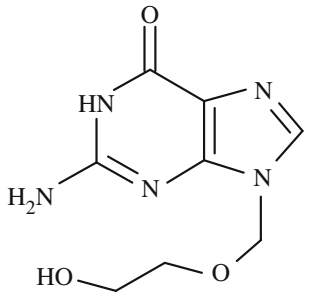

Scheme 1 Chemical structure of acyclovir

Based on an alteration of their thymidine kinase, HSV and VZV may develop resistance to acyclovir, particularly in immunocompromised patients.

Drug analysis has an extensive impact on public health. Several analytical methods have been developed for the quantitative determination of drugs in both pharmaceutical and biological samples. Electrochemical techniques have been used for the determination of a wide range of drug compounds, often without derivatization [3–8]. Additionally, electrochemical techniques include the determination of the drug-based electrode mechanism. Redox properties of drugs can provide insight into their metabolic fate, their in vivo redox processes, and their pharmacological activity [9,10].

Chemically modified electrodes (CMEs) have attracted attention of many researchers [3–5, 10–12], mainly because the possibility of tuning the electrochemical reactivity of the modified electrode to a specific end, both by choosing appropriate modifier and by controlling the modification procedure. In order to modify electrodes, it can be immobilized redox agents in the bulk of the electrode material. Such agents mediate the electron transfer and determine the kinetics process between the mediator and the external chemical species [13]. The electrochemical methods using CMEs have been widely used as sensitive and selective analytical methods for the detection of the trace amounts of biologically important compounds [10, 12, 14, 15]. One of the most important properties of CMEs has been their ability to catalyze the electrode process via significant decreasing of overpotential with respect to the unmodified electrode. In addition, direct electron transfer process on bare surfaces is limited by the slow kinetics and surface fouling due to the adsorption of reaction product(s)/intermediate(s) in which cyclic potentials or electrode renewing are required to remove the adsorbed species [16, 17]. The redox mediators immobilized on the modified electrode surface can overcome the low sensitivity, reproducibility, and electrode fouling.

Modification of the carbon paste electrodes (CPEs) is accomplished by diverse modifiers. The dispersion of metal particles in the bulk of carbon paste characterized by strong attachment of metal particles to the graphite substrate, offers a homogeneous and stable introduction of the catalytic metal centers into the bulk of the electrode matrix. The metal particles-modified carbon paste electrodes possess both advantages of carbon pastes and electrocatalytic activity of metal surfaces.

CMEs based on copper and copper species have been proved to be electrocatalytically active for oxidation/reduction processes and analytical applications in recent years. These include application of copper bulk metal [18, 19], copper nanoparticles [14, 20], copper alloys [21], and copper complexes [22].

Nanostructured materials have raised research interests among multidisciplinary researches in the last few years due to comparable characteristic length scales with the critical length scales of physical phenomena [23, 24]. In comparison with bulk materials, nanostructured materials exhibit interesting and peculiar properties, e.g. size- and shape-dependent and catalytic activities, novel mechanical properties, unique magnetic phenomena, crystal-shape-dependent thermodynamics, and quantum confinement phenomena [25]. It is well known that such unique properties and improved performances are determined by their size, structure, and mutual interaction among the nanostructured species [26].

Application of nanostructured materials has recently attracted electrochemical researches. Owing to the small size, nanoparticles exhibit unique physicochemical properties which are not represented by their bulk forms [27, 28]. Electrochemistry can cover the wide extent of nanoparticle investigations ranging from nanoparticle preparation to electrochemical sensor application and from band gap determination to photonic cell operation. Many types of nanoparticles including metal, oxide, semiconductor and composite nanoparticles have been greatly used in electrochemical studies [14, 20, 29, 30]. Nanoparticles display unique advantages over micro- and macro-structured materials when used for electroanalysis: enhancement of mass transport, catalysis, high effective surface area, and control over the electrode microenvironment [31].

Building on our recent studies on the application of modified electrodes for oxidation and determination of some drugs and biologically active compounds [3–5, 11, 12, 14, 15, 18, 20, 29, 30], in this work, the electrocatalytic oxidation of acyclovir on a copper nanoparticles-modified carbon paste electrode was investigated.

Materials and methods

Chemicals

All chemicals used in this work were of analytical grade from Merck or Aldrich, and were used without further

purification. Copper microparticles with the diameter of <63 μm were obtained from Merck and copper nanoparticles were obtained from Aldrich. All solutions were prepared by redistilled water. Acyclovir was received as a gift from Arasto Pharmaceutical Chemicals, Tehran, Iran. The acyclovir tablets and topical cream were obtained from a local drugstore.

Instruments

Electrochemical measurements were carried out in a conventional three-electrode cell powered by a Potentiostat/Galvanostat, μ-Autolab, typeIII (Eco Chemie, Utrecht, The Netherlands). The system was run on a PC using GPES 4.9 software. A saturated Ag/AgCl and a platinum disk (both from Azar Electrode, Iran) were used as reference and counter electrodes, respectively.

Surface morphological studies were carried out using scanning electron microscopy (SEM), a X-30 Philips instrument. To obtain information about the morphology and size of particles, transmission electron microscopy (TEM) was performed using a CEM 902A ZEISS instrument with an accelerating voltage of 80 kV. Samples were prepared by placing a drop of the particles, dispersed in acetone, on a carbon-covered nickel grid (400 mesh) and evaporating the solvent.

Electrode preparation

Unmodified CPE (un-CPE) was prepared by hand-mixing carbon powder and mineral oil with an 80/20% (*w*/*w*) ratio. The paste was carefully mixed and homogenized in an agate mortar for 20 min. The resulting paste was kept at room temperature in a desiccator before use. The paste was packed firmly into a cavity (4.05 mm diameter, geometric surface are of 0.128 cm^2 and 0.5 mm depth) at the end of a Teflon tube. Electrical contact was established via a copper wire connected to the paste in the inner hole of the tube. The electrode surface was gently smoothed by rubbing on a piece of weighing paper just prior to use. This procedure was also used to regenerate the surface of CPEs. The copper microparticles and copper nanoparticles-modified carbon paste electrodes (denoted as micro-CPE and nano-CPE, respectively) were prepared by mixing carbon powder, copper micro- or nanoparticles, and mineral oil with a 60/20/20% (*w*/*w*) ratio. nano-CPE covered with Nafion was prepared by applying 10 μL of a 5% *w*/*v* low aliphatic alcohols Nafion solution.

Procedures

Standard solutions of authentic drug were prepared by dissolving an accurate mass of the bulk drug in an appropriate volume of 100 mM NaOH solution (which was also used as supporting electrolyte) and then stored in the dark at 4 ºC. Additional dilute solutions were prepared daily by accurate dilution just before use. The drug solutions were stable and their concentrations did not change with time.

In order to compare the currents measured with micro-CPE and nano-CPE, the effective surface areas of the electrodes were determined. Based on the reported mechanism (vide infra), acyclovir is oxidized on the active sites of copper placed on the electrode surface. Therefore, the anodic currents must be normalized with respect to the total coverage area of copper active sites. To obtain such effective surface areas, the anodic charge passed for the oxidation of copper species was measured in alkaline solution for the modified electrodes; these values were related directly to the effective surface areas. Accordingly, the currents in the cyclic voltammograms were reported as current densities which they normalized with respect to the effective surface areas.

The calibration curve for the drug in 100 mM NaOH solution was measured with an amperometric technique. Working potential of 730 mV was used in amperometric measurements, in which the transient currents were allowed to decay to steady-state values.

For analysis of the drug tablets, the average weight of five tablets from each sample was determined; then the tablets were finely powdered and homogenized in a mortar. Appropriate accurately weighed amounts of the homogenized powder were transferred into 100-mL calibrated flasks containing 50 mL of 100 mM NaOH solution. The contents of the flasks were sonicated for 30 min and then the undissolved excipients were removed by filtration and diluted to volume with the same supporting electrolyte. Appropriate solutions were prepared by taking suitable aliquots of the clear filtrate and diluting them with 100 mM NaOH solution.

For analysis of topical cream, a suitable amount of cream transferred into a beaker, then 50 ml of 100 mM NaOH solution was added. The contents of the beaker were sonicated for 30 min and then the undissolved excipients were removed by filtration. Appropriate solutions were prepared by taking suitable aliquots of the clear filtrate and diluting them with 100 mM NaOH solution. All studies/measurements were carried out at room temperature.

Results and discussion

Surface morphology studies

Figure 1 represents SEM (a) and TEM (b) images of copper nanoparticles. Spherical nanoparticles of copper and also

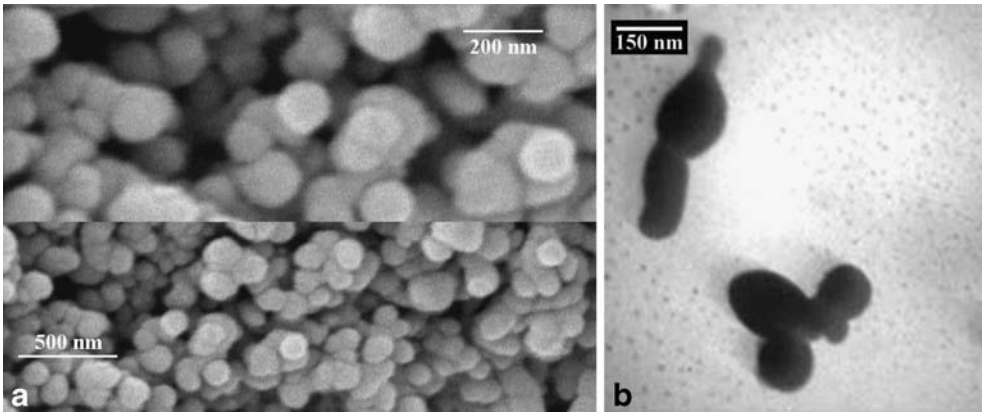

Fig. 1 Scanning electron micrographs (**a**) and TEM images (**b**) of copper nanoparticles

some particle aggregations were clearly observed. Copper particles with near-spherical shape with an average diameter of 90 nm can be observed.

Cyclic voltammetric studies

Figure 2 shows typical cyclic voltammograms of un-CPE (curve a), micro-CPE (curve b), and nano-CPE (curve c) recorded in 100 mM NaOH solution in the potential range of 0–900 mV using a potential sweep rate of 10 mV s^{-1}. In the case of un-CPE, only the discharge current of the solvent is observed at the anodic edge of the voltammogram. Voltammograms of micro-CPE and nano-CPE are in good agreement with those reported in the literature for copper-based electrodes [32–34]. It is believed that the charge passed at the onset of the anodic decomposition of the solvent presumably corresponds to the Cu(II)/Cu(III) redox transition [32, 35, 36]. It always occurred in the course of the oxidation of copper- and copper-containing modified electrodes [37]. The presence of Cu(II)/Cu(III) redox transition at the anodic edge of the voltammograms is also reported by Miller [38] for a ring-disk voltammetric study of copper electrodes in alkaline solutions. It should be noted that the characteristics of the voltammograms of copper in alkaline solutions strongly depend on pH, potential sweep rate, mass transport regime, as well as other experimental conditions. Their complex appearance originates from the complexity of the reaction mechanism. In addition, upon prolonged potential cycling, different copper oxide species were formed on the copper surface [18, 20]. Regarding the nature of Cu(III) entity, species ranging from copper oxyhydroxide to Cu(III) radical have been proposed [37, 39]. It has been reported that copper can oxidize organic compounds by chemical reactions between Cu(III) active species and those compounds via a redox mediation electron transfer process (mediated electrocatalytic reaction, EC' mechanism) at the anodic edge of the voltammograms in alkaline solutions [14, 18, 20, 37–39]. It should be also noted that the current density for nano-CPE is higher than micro-CPE (curve c vs. curve b).

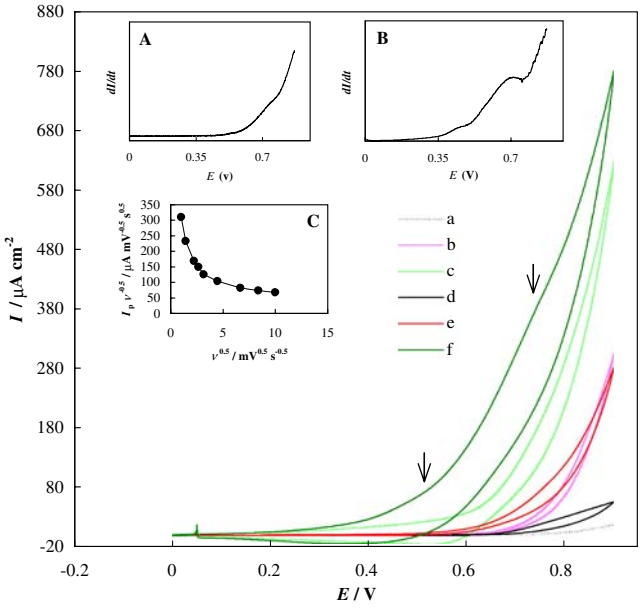

Fig. 2 *Main panel* Cyclic voltammograms of un-CPE (*a*, *d*), micro-CPE (*b*, *e*) and nano-CPE (*c*, *f*) in the potential range of 0–900 mV in 100 mM NaOH solution in the absence (*a*, *b*, *c*) and presence (*d*, *e*, *f*) of 5.0 mM acyclovir. The potential sweep rate was 10 mV s^{-1}. *Inset A* Derivative voltammogram of the electrocatalytic oxidation of acyclovir on micro-CPE (curve *e*). *Inset B* Derivative voltammogram of the electrocatalytic oxidation of acyclovir on nano-CPE (curve *f*). *Inset C* Current function vs. square root of the potential sweep rate. The data obtained from cyclic voltammograms of nano-CPE recorded at different potential sweep rates in the presence of acyclovir. The *arrows* indicate the locations of anodic peaks

Cyclic voltammograms of un-CPE (curve d), micro-CPE (curve e), and nano-CPE (curve f) recorded in the presence of 5.0 mM acyclovir are also represented in Fig. 2. While acyclovir represented very weak oxidation signal on un-CPE, it was oxidized on both micro-CPE and nano-CPE surfaces. On the micro-CPE surface, it was oxidized via a single anodic peak. It was further confirmed

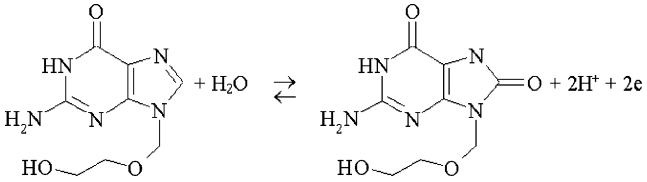

Scheme 2 Oxidation of acyclovir to the corresponding oxo-guanine analog

by the corresponding derivative voltammogram (the current derivative with respect to time vs. potential) (Fig. 2, inset A). On nano-CPE surface, however, it was oxidized via two overlapped anodic peaks located at 600 and 730 mV followed by a decrease in the cathodic peak current in the reverse sweep. The anodic peaks appeared in the voltammograms of nano-CPE in the presence of the drug (indicated with two arrows) can be better visualized when the derivative voltammogram is looked at (Fig. 2, inset B). In addition, in the case of nano-CPE, it can be deduced that the anodic current density related to the electrooxidation of the drug is higher compared to micro-CPE. It can be related to the nanosize effect of the copper nanoparticles which have higher reactivity compared to those of micro-size because the currents were normalized for the effective surface areas of the electrodes (vide supra). Another point in Fig. 2 is that the onset potential of acyclovir electrooxidation on nano-CPE shifted in negative direction compared to micro-CPE, and accordingly, the electrooxidation of acyclovir on nano-CPE occurred at lower potentials. This behavior indicates that nanoparticles of copper caused the oxidation process to be occurred at favorable potentials. Therefore, nanoparticles of copper performed the electrooxidation process of acyclovir better than those of microparticles both from kinetics and from thermodynamics points of view.

From cyclic voltammograms depicted in Fig. 2, it can be summarized that acyclovir was oxidized on copper-based electrodes in the potential region of formation of active Cu(III) species, while the cathodic currents in the reverse sweep were diminished. In addition, cyclic voltammograms were recorded using nano-CPE in the presence of the drug at different potential sweep rates (data not shown). Then, the current function (peak current divided by the square root of the potential sweep rate) against the square root of the potential sweep rate was plotted (Fig. 2, inset C). This plot reveals negative slope and confirms a cyclic mediated redox mechanism via Cu(III) species in an EC' mechanism. Copper species were immobilized on the electrode surface and the one with a higher valence oxidized acyclovir via a chemical reaction followed by generation of low-valence copper. This species was generated at positive potentials and has been reported to play the role of a redox mediator in the oxidation of some compounds on copper-based electrodes [18, 20, 32, 37–39]. Therefore, the electrode reaction may proceed via a mechanism containing a rate-limiting step in which intermediates/products species are formed upon chemical reaction of acyclovir with Cu(III) species. Then, the surface regenerates through chemical redox reaction(s). Based on the results, the following mechanism can be proposed for the mediated oxidation of the drug on the modified surface. The redox transition of the copper species:

$$\mathrm{Cu(II)} \rightleftarrows \mathrm{Cu(III)} + \mathrm{e} \tag{1}$$

is followed by the oxidation of acyclovir on the modified surface via the following reactions:

$$\mathrm{Cu(III)} + \mathrm{Acyclovir} \overset{k_{\mathrm{cat1}}}{\rightarrow} \mathrm{Intermediate/Pr\,oduct\ 1} + \mathrm{Cu(II)} \tag{2}$$

$$\mathrm{Cu(III)} + \mathrm{Intermediate/Pr\,oduct\ 1} \overset{k_{\mathrm{cat2}}}{\rightarrow} \mathrm{Pr\,oduct\ 2} + \mathrm{Cu(II)} \tag{3}$$

The anodic current generated for the acyclovir electrooxidation process can be attributed to the oxidation of one electroreactive functional group in multiple steps and/or simultaneous oxidation of electroreactive functional groups present in the acyclovir structure. Herein, as a guanine analog, acyclovir can be oxidized to the corresponding oxo-guanine analog according to the reaction shown in

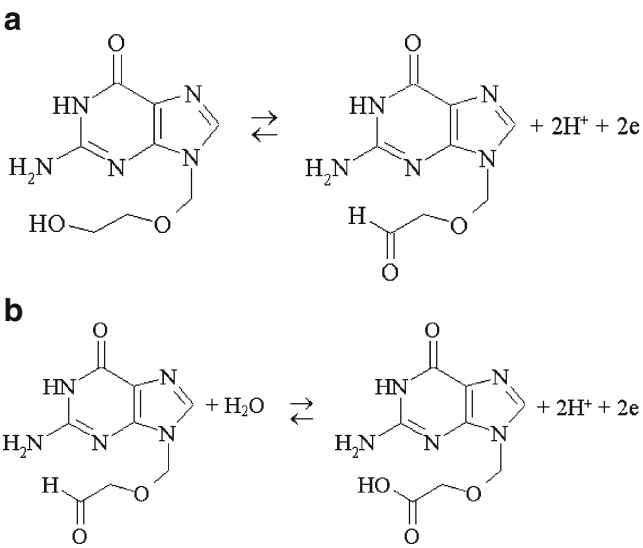

Scheme 3 Oxidation of acyclovir to the corresponding aldehyde (*A*) and/or carboxylic acid (*B*)

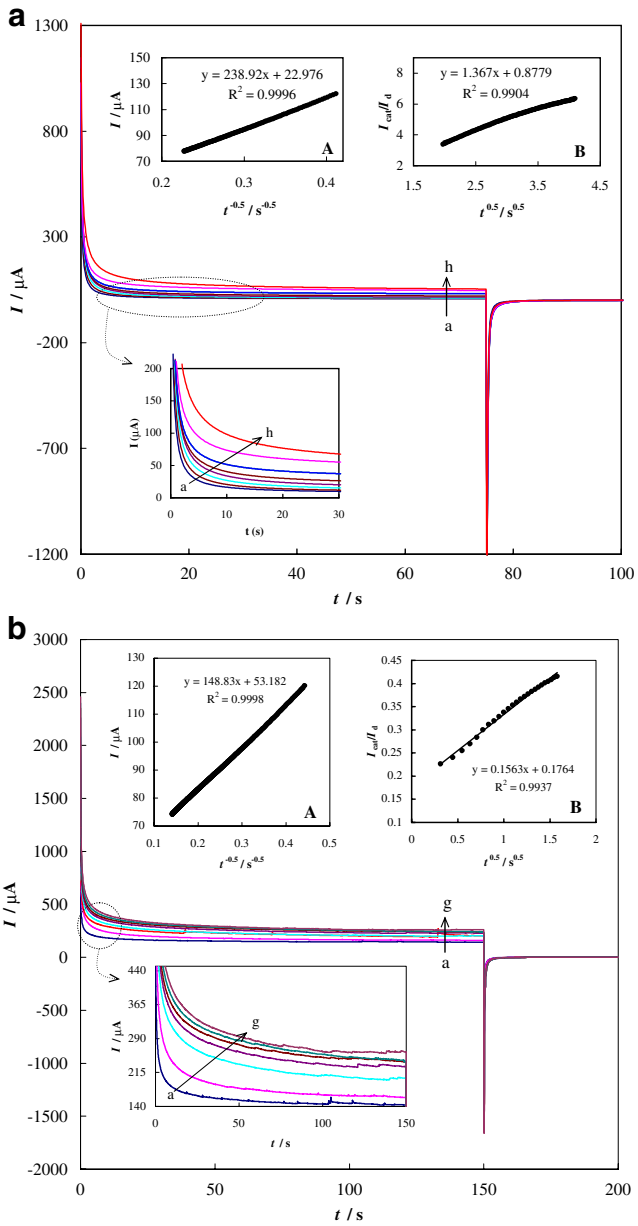

Fig. 3 **a** *Main panel* Double-step chronoamperograms of nano-CPE in 100 mM NaOH solution with different concentrations of acyclovir of (a) 0, (b) 0.17, (c) 0.26, (d) 0.53, (e) 0.95, (f) 2.13, (g) 4.61, and (h) 5.12 mM. Potential steps were 600 mV and 200 mV, respectively. *Inset A* Dependency of transient current on $t^{-0.5}$. *Inset B* Dependence of I_{catal}/I_d on $t^{0.5}$. **b** *Main panel* Double-step chronoamperograms of nano-CPE in 100 mM NaOH solution with different concentrations of acyclovir of: (a) 0, (b) 1.0×10^{-4}, (c) 0.43, (d) 0.85, (e) 1.37, (f) 2.03, and (g) 3.09 mM. Potential steps were 730 and 300 mV, respectively. *Inset A* Dependency of transient current on $t^{-0.5}$. *Inset B* Dependence of I_{catal}/I_d on $t^{0.5}$

Scheme 2 [40, 41] and it can also be oxidized, as a primary alcohol, to the corresponding aldehyde and/or carboxylic acid via the reactions shown in Scheme 3 [42]. However, it should be emphasized that the exact entity of the product(s) of the electrooxidation reaction is out of the scope of this study. It needs further investigation using other coupled analytical techniques.

Another point seen in Fig. 2 is that no anodic peak is regenerated in the reverse (negative) sweep which may be observed in the course of anodic processes of organic compounds on the modified electrode surfaces [15, 19]. In a separate experiment, consecutive cyclic voltammograms were recorded in the presence of 5.0 mM acyclovir using nano-CPE (data not shown). It was deduced finally that near the same voltammograms were attained. These results indicate that the copper nanoparticle surfaces are resistant to be fouled up by the product(s)/intermediate(s) of the electrooxidation reaction; electrode fouling, a common and serious limitation observed for the sensors based on direct electron oxidation of acyclovir [16], did not take place here. This confirms the reproducibility and robustness of nano-CPE.

Chronoamperometric studies

Chronoamperometry was also employed for the investigation of the processes occurred via the EC' mechanism [43] on nano-CPE. Figure 3 shows double-step chronoamperograms for nano-CPE both in the absence and in the presence of acyclovir over a wide concentration range. Two sets of chronoamperograms were recorded which the applied potential steps were 600 and 200 mV respectively in Fig. 3a and 730 and 300 mV respectively in Fig. 3b. The

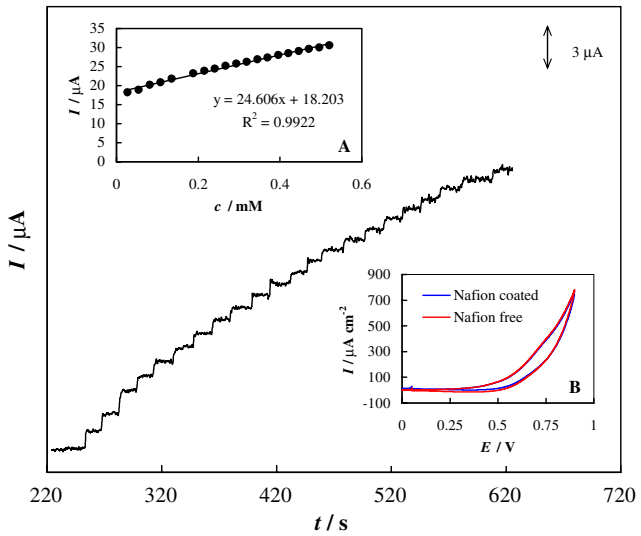

Fig. 4 *Main panel* Current signal as a function of time in 100 mM NaOH solution during repetitive injections of acyclovir using nano-CPE. Applied potential was 730 mV. *Inset A* Dependency of the transient current on acyclovir concentration using nano-CPE. *Inset B* Cyclic voltammograms of uncoated and coated nano-CPE with Nafion membrane in 100 mM NaOH solution in the presence of 5.0 mM acyclovir. The potential sweep rate was 10 mV s^{-1}

Table 1 The determined parameters for calibration curve of drug and accuracy and precision (n=10) for electrocatalytic oxidation of acyclovir on nano-CPE

Linear range (μM)	27–521
Slope (mA M^{-1})	24.6±0.2
Intercept (μA)	18.2±0.1
LOD (μM)	2.64
LOQ (μM)	8.82
RSD (%)[a]	2.75
RSD (%)[b]	4.23
Bias (%)[c]	0.5

[a] Within day reproducibility

[b] Between day reproducibility

[c] The value was reported for the middle concentration of the calibration curve (1.62×10^{-4} M)

transient currents increase upon raising acyclovir concentration and when the potential step jumped to the reverse values, no significant currents are obtained indicating irreversibility of the processes. Plotting the net currents versus the minus square roots of time results in linear dependencies in Cottrellian manners (Fig. 3, insets A). This indicates that the two steps of the electrocatalytic oxidation of acyclovir on nano-CPE are controlled by diffusion in the bulk of solution. By using the slope of the line represented in Fig. 3a, inset A, the diffusion coefficient of the drug can be obtained according to the Cottrell equation [43]

$$I = nFAD^{1/2}c\pi^{-1/2}t^{-1/2} \tag{4}$$

where I is the transient current, n is the number of the exchanged electrons, A denotes the electrode surface area, D stands for the diffusion coefficient of the electroreactive species, c is the bulk concentration, and t is the elapsed time. The mean value of the diffusion coefficient for acyclovir was found to be $1.68 \pm 0.03 \times 10^{-5}$ cm^2 s^{-1}. This value is in good agreement with what has reported in the literature [16]. We used only chronoamperogram recorded at 600 mV which corresponds to the first step of electrocatalytic oxidation of acyclovir. This is due to uncertainty of the concentration for the second step of the oxidation reaction.

Chronoamperometry can also be used to evaluate the catalytic rate constant according to the following equation [43]:

$$I_{cat}/I_d = \gamma^{1/2}\left[\pi^{1/2}\mathrm{erf}\left(\gamma^{1/2}\right) + \exp(-\gamma)/\gamma^{1/2}\right] \tag{5}$$

where I_{cat} and I_d are the currents in the presence and absence of the drug, respectively, and $\gamma=k_{cat}ct$ is the argument of the error function. k_{cat} is the catalytic rate constant and t is the elapsed time. In the cases where $\gamma>$ 1.5, erf($\gamma^{1/2}$) is almost equal to unity and Eq. 5 can be reduced to:

$$I_{cat}/I_d = \gamma^{1/2}\pi^{1/2} = \pi^{1/2}(k_{cat}ct)^{1/2} \tag{6}$$

From the slope of the I_{cat}/I_d versus $t^{1/2}$ plot which is presented in Fig. 3a, inset B, the mean value of catalytic rate constant for the first step of the oxidation reaction was obtained as $k_{cat1} = 1.16 \pm 0.02 \times 10^5$ cm^3mol^{-1} s^{-1}. Using similar approach with the linear plot represented in Fig. 3b, inset B, the value of catalytic rate constant for the second step of the oxidation reaction multiplied by the concentration is obtained as $c \times k_{cat2} = 3.35 \pm 0.05 \times 10^{-2}$ s^{-1}.

Analytical part

In order to develop a simple and time-saving method for the analysis of acyclovir in pure form as well as pharmaceutical

Table 2 Determination and recovery of acyclovir in pharmaceutical forms

Sample type	Amount labeled	Amount added	Amount found	Recovery (%)	RSD (%)	Bias (%)
Tablet-sample 1	200 mg	–	201 mg	100.50	3.31	0.50
Tablet-sample 1	–	200 mg	212 mg	106.00	3.61	6.00
Tablet-sample 1	–	200 mg	207 mg	103.50	3.71	3.50
Tablet-sample 2	200 mg	–	197.5 mg	98.75	3.15	−1.25
Tablet-sample 2	–	200 mg	195 mg	97.50	3.25	−2.50
Tablet-sample 2	–	200 mg	193 mg	96.50	3.18	−3.50
Tablet-sample 3	200 mg	–	193 mg	96.50	3.66	−3.50
Tablet-sample 3	–	200 mg	199 mg	99.50	3.69	−0.50
Tablet-sample 3	–	200 mg	198 mg	99.00	3.78	−1.00
Topical cream	5%	–	5.02%	100.40	3.42	0.40
Topical cream	–	5%	5.04%	100.80	3.56	0.80
Topical cream	–	5%	5.05%	101.00	3.59	1.00

formulations, amperometry technique was used. Typical amperometric signals obtained during successive increments of acyclovir to a 100 mM NaOH solution using nano-CPE are depicted in Fig. 4. Gentle stirring for a few seconds was needed to promote solution homogenization after each injection. The electrode response was quite rapid and proportional to the acyclovir concentration. The corresponding calibration curve for the amperometric signals is shown in inset A of Fig. 4. The limit of detection (LOD) and quantitation (LOQ) of the procedure were calculated according to the 3 SD/*m* and 10 SD/*m* criteria, respectively, where SD is the standard deviation of the intercept and *m* is the slope of the calibration curve [44]. The determined parameters for the calibration curve of the drug, accuracy and precision, LOD and LOQ, and the slope of calibration curve are reported in Table 1.

The applicability of the proposed amperometric method for the sample dosage forms was examined by analyzing the tablets and topical cream. It was found that the amounts of the drug determined using this method are in good agreement with the reported values. The values of experimentally determined drugs and declared values in tablets and topical cream are tabulated in Table 2.

In order to evaluate the accuracy of this method and to know whether the excipients in pharmaceutical dosage forms show any interference with the analysis, the proposed amperometric method was checked by recovery experiments using the standard addition method. After addition of known amounts of pure drug to various pre-analyzed formulations of acyclovir, the mixtures were analyzed by the proposed method. The recovery of acyclovir was calculated using the corresponding regression equations of previously plotted calibration plots. The results of recovery experiments using the developed assay procedure are presented in Table 2. The results indicate the absence of interference from commonly encountered pharmaceutical excipients used in the selected formulations. Therefore, the method can be applied to the determination of acyclovir in pharmaceutical forms without any interference from inactive ingredients.

In order to investigate the selectivity of the method, the interference effects of some biologically important compounds were tested. The effects of guanine, adenine, and xanthine are serious. These compounds have similar electroreactive functional groups and are oxidized at the potentials close to that of acyclovir. It was observed that when a Nafion membrane was applied to the top of nano-CPE surface, the response of the electrode towards acyclovir remains almost unchanged (cyclic voltammograms of uncoated and coated nano-CPE with Nafion in the presence of acyclovir are shown in inset B of Fig. 4). While, L-ascorbic acid, D-glucose, uric acid, L-cysteine, and ephedrine have almost no influences on the current responses of acyclovir, due to rejection of the diffusion of these anionic compounds by the membrane.

Conclusion

Carbon paste electrodes modified with particles of copper were employed for investigation of the electrocatalytic oxidation and determination of acyclovir. Acyclovir was oxidized on copper-based electrodes via mediation of Cu(III) active species. micro-CPE represented a single anodic peak in the voltammograms, while nano-CPE generated two anodic peaks with the higher corresponding currents located at lower potentials. It was related to the nanosize of copper nanoparticles; the nanoparticles of copper seemed to accelerate the electrooxidation process. Amperometric procedure was successfully applied using the nanoparticles for the quantification of acyclovir with high sensitivities in bulk and two forms of pharmaceutical samples.

Acknowledgments The financial support of the Iran National Science Foundation (INSF) and the Research Council of University of Tehran are gratefully acknowledged.

References

1. Fishman JA, Rubin RH (1998) N Engl J Med 338:1741. doi:10.1056/NEJM199806113382407
2. Villacian JS, Paya CV (1999) Transpl Infect Dis 1:50. doi:10.1034/j.1399-3062.1999.10106.x
3. Yadegari H, Jabbari A, Heli H, Moosavi-Movahedi AA, Karimian K, Khodadadi A (2008) Electrochim Acta 53:2907. doi:10.1016/j.electacta.2007.11.003
4. Hajjizadeh M, Jabbari A, Heli H, Moosavi-Movahedi AA, Shafiee A, Karimian K (2008) Anal Biochem 373:337. doi:10.1016/j.ab.2007.10.030
5. Hajjizadeh M, Jabbari A, Heli H, Moosavi-Movahedi AA, Haghgoo S (2007) Electrochim Acta 53:1766. doi:10.1016/j.electacta.2007.08.026
6. Gilpin RK, Pachla LA (2005) Anal Chem 77:3755. doi:10.1021/ac050580o
7. Yadegari H, Jabbari H, Heli H, Moosavi-Movahedi AA, Karimian K (2008) Chem Anal (Warsaw) 53:5
8. Yadegari H, Jabbari H, Heli H, Moosavi-Movahedi AA, Majdi S (2008) 19:1017
9. Ozkan SA, Uslu B, Senturk Z (2004) Electroanalysis 16:231. doi:10.1002/elan.200402828
10. Ozkan SA, Uslu B, Aboul-Enein HY (2003) Crit Rev Anal Chem 33:155. doi:10.1080/713609162
11. Majdi S, Jabbari A, Heli H, Yadegari H, Moosavi-Movahedi AA, Haghgoo S (2009) J Solid State Electrochem 13:407. doi:10.1007/s10008-008-0567-6
12. Majdi S, Jabbari A, Heli H (2007) J Solid State Electrochem 11:601. doi:10.1007/s10008-006-0205-0
13. Andrieux CP, Saveant J-M (1992) In: Murray RW (ed.), Molecular Design of Electrode Surfaces, Wiley, New York

14. Heli H, Hajjizadeh M, Jabbari A, Moosavi-Movahedi AA (2009) Biosens Bioelectron 24:2328. doi:10.1016/j.bios.2008.10.036
15. Majdi S, Jabbari A, Heli H, Moosavi-Movahedi AA (2007) Electrochim Acta 52:4622. doi:10.1016/j.electacta.2007.01.022
16. Wang F, Chen L, Chen XX, Hu SH (2006) Anal Chim Acta 576:17. doi:10.1016/j.aca.2005.12.023
17. Skrzypek S, Ciesielski W, Yilmaz S (2007) Chem Anal Warsz 52:1071
18. Hajjizadeh M, Jabbari A, Heli H, Moosavi-Movahedi AA (2008) Chem Anal (Warsaw) 53:429
19. Paixao TRLC, Corbo D, Bertotti M (2002) Anal Chim Acta 472:123. doi:10.1016/S0003-2670(02)00942-X
20. Heli H, Hajjizadeh M, Jabbari A, Moosavi-Movahedi AA (2009) Anal Biochem 388:81. doi:10.1016/j.ab.2009.02.021
21. Mho S, Johnson DC (2001) J Electroanal Chem 500:524. doi:10.1016/S0022-0728(00)00277-1
22. Makowski O, Strorka J, Kulesza PJ, Malik MA, Galus Z (2002) J Electroanal Chem 532:157. doi:10.1016/S0022-0728(02)00965-8
23. Jortner J, Rao CNR (2002) Pure Appl Chem 74:1491. doi:10.1351/pac200274091491
24. Wade TL, Wegrowe JE (2005) Eur Phys J Appl Phys 29:3. doi:10.1051/epjap:2005001
25. Brechignac C, Houdy P, Lahmani M (eds) (2007) Nanomaterials and Nanochemistry, Springer, Berlin
26. Wang ZL (2000) In: Characterization of Nanophase Materials, Wiley-VCH, New York
27. Zhang LD, Mu JM (2001) Nanoscale materials and nanostructures. Science, Beijing
28. Yu AM, Liang ZJ, Cho JH, Caruso F (2003) Nano Lett 3:1203. doi:10.1021/nl034363j
29. Houshmand M, Jabbari A, Heli H, Hajjizadeh M, Moosavi-Movahedi AA (2008) 12:1117
30. Heli H, Jabbari A, Majdi S, Mahjoub M, Moosavi-Movahedi AA, Sheibani S (2009) J Solid State Electrochem (in press). doi:10.1007/s10008-008-0758-1
31. Katz E, Willner I, Wang J (2004) Electroanalysis 16:19. doi:10.1002/elan.200302930
32. Colon LA, Dadoo R, Zare RN (1993) Anal Chem 65:476. doi:10.1021/ac00052a027
33. Kano K, Torimura M, Esaka Y, Goto M, Ueda T (1994) J Electroanal Chem 372:137. doi:10.1016/0022-0728(93)03252-K
34. Pyun CH, Park SM (1986) J Electrochem Soc 133:20242. doi:10.1149/1.2108333
35. Burke LD, Ahern MJG, Ryan TG (1990) J Electrochem Soc 137:553. doi:10.1149/1.2086496
36. Casella IG, Gatta M (2000) J Electroanal Chem 494:12. doi:10.1016/S0022-0728(00)00375-2
37. Fleischmann M, Korinek K, Pletcher D (1972) J Chem Soc, Perkin Trans 2:1396. doi:10.1039/p29720001396
38. Miller B (1969) J Electrochem Soc 116:1675. doi:10.1149/1.2411657
39. Meyerstein D, Hawkridge FM, Kuwana T (1972) J Electroanal Chem 40:377. doi:10.1016/S0022-0728(72)80382-6
40. Honeychurch KC, O'Donovan MR, Hart JP (2007) Biosens Bioelectron 22:2057. doi:10.1016/j.bios.2006.09.019
41. Gonzalez-Fernandez E, de-los Santos-Alvarez N, Lobo-Castanon MJ, Miranda-Ordieres AJ, Tunon-Blanco P (2008) Electroanalysis 20:833. doi:10.1002/elan.200704153
42. Hammerich O, Utley JHP, Eberson L (eds) (1991) Organic electrochemistry. Marcel Dekker, New York
43. Bard AJ, Faulkner LR (2001) Electrochemical methods. Wiley, New York
44. Miller JC, Miller JN (1994) Statistics for analytical chemistry, 4th edn. Ellis-Harwood, New York, p 115